Solubilities of L-Proline in Subcritical HFC-134a and Supercritical CO_2 Fluids†

Ling Liu, Zhen Li, Zhong-Wen Liu, and Zhao-Tie Liu*

Key Laboratory of Applied Surface and Colloid Chemistry (Shaanxi Normal University), Ministry of Education, Xi'an 710062, People's Republic of China, and School of Chemistry and Materials Science, Shaanxi Normal University, Xi'an 710062, People's Republic of China

A static method coupled with gravimetric analysis was used to measure the solubility of L-proline in subcritical 1,1,1,2-tetrafluoroethane (HFC-134a) and supercritical CO_2 ($scCO_2$). The solubility of L-proline is much higher in HFC-134a fluid than in $scCO_2$. The solubilities of L-proline in HFC-134a and $scCO_2$ are affected by temperature and pressure. The solubilities increase with increasing temperature and pressure for both $scCO_2$ and HFC-134a solvents. The densities of $scCO_2$ and subcritical HFC-134a were calculated using the Peng−Robinson (P-R) equation. Experimentally determined density data were used to assess the accuracy of the P-R equation.

Introduction

In recent decades, L-proline, the simplest "protein",[1] has become one of the most attractive molecules in green synthetic chemistry because it is an inexpensive and readily available amino acid. As an effective organocatalyst,[2] it has been successfully applied to a variety of reactions[3] of which the direct aldol reaction is particularly interesting.[4] L-proline suffers from a number of problems that reduce its attractiveness as a catalyst:[5] (1) poor solubility in most solvents except water (where it functions as a catalyst, but without enantioselectivity); (2) potential side reactions such as oxazolidinone formation, decarboxylation, and subsequent [3 + 2] cycloaddition reactions; and (3) most of the L-proline-catalyzed aldol reactions have been carried out in organic media such as DMF and DMSO.[6] Large amounts of organic solvents are used in chemical reactions, most of which are volatile, toxic, and flammable. From the viewpoint of greener processes, the use of nonhazardous and renewable materials is one of the most important goals of green chemistry.

The advantages of supercritical fluids (SCF) compared with conventional liquid solvents include low surface tension, high diffusivity, low viscosity, and high compressibility. In addition, the density, dielectric constant, diffusion coefficient, and solubility parameter can be tuned continuously by varying pressure and temperature. For those reasons supercritical fluids have become attractive solvents for many industrial processes including extraction,[7] polymer processing,[8] phase transfer reactions and catalysis,[9] enzymatic catalysis,[10] processing of microelectronic devices,[11] and synthesis of nanoparticles.[12−15]

Supercritical carbon dioxide ($scCO_2$) is the most popular solvent among SCFs due to its nontoxicity, nonflammability, low cost, ready availability, and near-ambient critical temperature. Unfortunately, because CO_2 is a nonpolar solvent with weak van der Waals forces it is not suitable for dissolving polar substances. That disadvantage has limited its application to separation, reaction, and material formation processes. Fortunately, polar substances can easily dissolve in fluorohydrocarbons such as chlorodifluoromethane (HCFC-22), trifluoromethane (HFC-23), difluoroethane (HFC-32), pentafluoroethane (HFC-125), 1,1,1,2-tetrafluoroethane (HFC-134a), and 1,1,1-trifluoroethane (HFC-143a).[16−23]

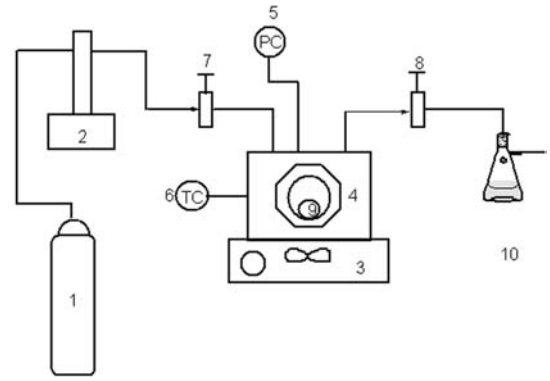

Figure 1. Schematic diagram of experimental setup. 1, Carbon dioxide cylinder; 2, ISCO model 260D syringe pump; 3, magnetic stir device; 4, SF-400 high-pressure vessel; 5, pressure transducer; 6, thermocouple assembly; 7, intake valve; 8, back pressure valve; 9, sample vial; 10, reclaimer vase.

Generally, two techniques, the flowing method and the static method, are used to measure solubility in SCFs. Calculations of solubility are correlated using a mathematical model such as the semiempirical model proposed first by Bartle, which was subsequently used successfully by others, the model proposed by Chrastil, and some equations, such as the Peng−Robinson (P-R) and the Soave−Redlich−Kwong (S-R-K) equations.[24−29]

In the present study, a static method coupled with gravimetric analysis[30] was developed for measuring the solubility of solids in $scCO_2$ and HFC-134a. The densities of $scCO_2$ and HFC-134a, which are functions of temperature and pressure, were also simulated with the P-R equation. Experimentally determined density data were used to assess the accuracy of the P-R equation, which will provide useful data for future applications of the aldol reaction in SCFs.

Experimental Section

Materials and Instruments. CO_2 was obtained from Xi'an Yatai Liquid Gas Co., and 1,1,1,2-tetrafluoroethane (HFC-134a)

* To whom correspondence should be addressed. E-mail: ztliu@snnu.edu.cn. Fax: +86 29 85303682.
† Part of the "William A. Wakeham Festschrift".

10.1021/je801009z CCC: $40.75
Published on Web 04/22/2009

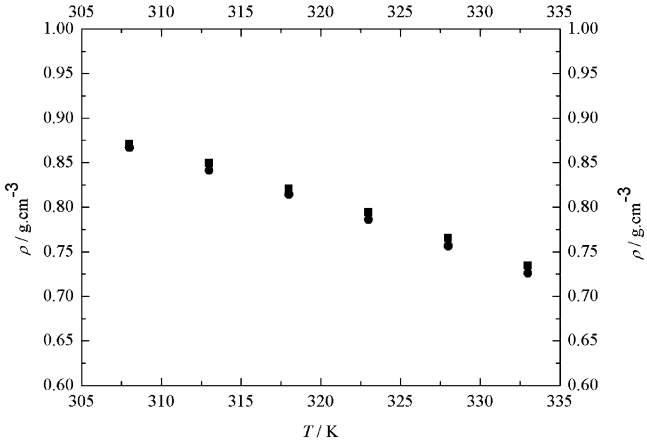

Figure 2. Density of $scCO_2$ calculated by the P-R equation and determined experimentally at 20 MPa and a range of temperatures. ■, experimental data (density of our work); ●, P-R equation data (density of P-R equation).

(99.9%) was obtained from Xi'an Jinzhu Modern Chemical Industry Co., Ltd. L-proline (chromatography pure) was purchased from Sinopharm Group Chemical Reagent ShanghaiCo., Ltd. The reagents used in this study were analytically pure grade chemicals. All chemicals were used without further purification.

A schematic diagram of the experimental setup for solubility measurements is given in Figure 1.

Measurements of Solubility. For each experiment, an excess amount of solute and a small magnetic stirring bar were placed in a glass vial (16 mL) that was then capped with a coarse filter paper attached to the vial with Teflon tape. The sample vial was weighed (W_1) and placed inside the pressure vessel.

The pressure vessel was sealed and weighed (M_1) and then heated to the desired temperature by a heater via a machined internal heating rod. When the desired temperature was reached, stirring was initiated and the vessel was slowly filled with CO_2 or HFC-134a until the desired pressure was achieved. The vessel was then reweighed (M_2). After sufficient time (usually at least 24 h, as reported previously[31]) for HFC-134a/solute or CO_2/solute dissolution equilibrium to be attained, the vessel was depressurized and opened. The vial was removed, wiped with a clean tissue, dried, and reweighed (W_2). The solubility of the solute was then given by the following equation

$$\text{Solubility (wt/vol)} = \frac{W_1 - W_2}{V_1 - V_2} \tag{1}$$

where W_1 and W_2 are the initial and final mass of solute in the vial, V_1 (59 mL) is the volume of the high-pressure vessel, and V_2 (16 mL) is the volume of vial. This equation incorporates a correction factor that accounts for precipitation of the solute in the fluid phase in the vial. The volume of the vessel in this equation is the volume accessible to the fluid phase which was determined to be 43 mL.

The Foundation of the P-R Equation. Although it has obvious disadvantages, the P-R equation gives an appropriate qualitative description and superior accuracy of quantitative calculation for the phase behavior of supercritical fluids. The P-R equation can apply to many complex systems based on supercritical fluids. In previous work,[32] we have derived a P-R equation.

The standard form of the P-R equation[29,33] is

$$P = \frac{RT}{V - b} - \frac{a}{V(V + b) + b(V - b)} \tag{2}$$

The Measurement and Calculation of Pure CO_2 and HFC-134a Density. The calculation methods for pure CO_2 or HFC-134a density for the measurement system are given in eqs 3 and 4.

The density, ρ, of CO_2 or HFC-134a in the high pressure vessel is then

$$\rho = \frac{m}{V_{\text{vessel}}} \tag{3}$$

or

$$\rho = \frac{n}{V_{\text{vessel}}} \tag{4}$$

Results and Discussion

Model Analysis. The equations used to calculate standard deviation (s) and absolute error (d) are as follows

$$s = \sqrt{\frac{\sum (x - \bar{x})^2}{n - 1}} \tag{5}$$

$$d = x - \bar{x} \tag{6}$$

where $n - 1$ is the degrees of freedom.

The density data from the P-R equation and measured for $scCO_2$ at 20 MPa and varying temperature are given in Figure 2. The analysis of these data is shown in Table 1. The standard deviation of the measured density was 0.0515 g·cm^{-1}, and the standard deviation of the density calculated using the P-R equation was 0.0528 g·cm^{-1}. The density data from P-R equation and the data measured for HFC-134a at 19.6 MPa and varying temperature are given in Figure 3. The analysis of these data is shown in Table 2. The standard deviation of the measured density was 0.0474 g·cm^{-1}, and the standard deviation of the density calculated by P-R equation was 0.0564 g·cm^{-1}. At the same pressure, the density curve from the P-R equation for $scCO_2$ or HFC-134a is nearly parallel to the corresponding measured density curve. The two standard deviations are very similar which indicates that the P-R equation is accurate for use in our experimental calculation.

The density from the P-R equation and the density measured for $scCO_2$ at 313 K and varying pressure are shown in Figure 4. The analysis of the density data is shown in Table 3. The curve of measured density tends toward the curve of density calculated by the P-R equation when the pressure is between 15 and 25 MPa. The two curves deviate from each other gradually at lower and higher pressures. The standard deviation

Table 1. Standard Deviation and Absolute Error of CO_2 Density Calculated Using the P-R Equation and Experimentally Determined at 20 MPa and a Range of Temperatures[a]

T	ρ_1	ρ_2	d_1	d_2	s_1	s_2
K	g·cm^{-3}	g·cm^{-3}	g·cm^{-3}	g·cm^{-3}	g·cm^{-3}	g·cm^{-3}
308	0.87 ± 0.06	0.8669	0.0654	0.0684	0.0515	0.0528
313	0.85 ± 0.04	0.8412	0.0434	0.0427		
318	0.82 ± 0.01	0.8143	0.0147	0.0158		
323	0.79 ± 0.01	0.7860	−0.0116	−0.0124		
328	0.76 ± 0.04	0.7565	−0.0403	−0.0419		
333	0.73 ± 0.07	0.7258	−0.0715	−0.0726		

[a] ρ_1, experimentally determined density; ρ_2, density from P-R equation; d_1, absolute error of experimental density; d_2, absolute error of density from P-R equation; s_1, standard deviation of experimental density; s_2, standard deviation of P-R equation density.

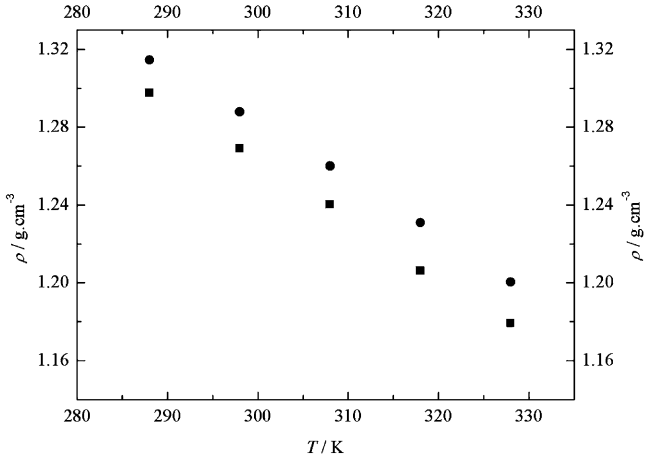

Figure 3. Density of HFC-134a calculated using the P-R equation and determined experimentally at 20 MPa and a range of temperatures. ■, experimental data (density of our work); ●, P-R equation data (density of P-R equation).

Table 2. Standard Deviation and Absolute Error of HFC-134a Density Calculated Using the P-R Equation and Experimentally Determined at 19.6 MPa and a Range of Temperatures[a]

T	ρ_1	ρ_2	d_1	d_2	s_1	s_2
K	g·cm^{-3}	g·cm^{-3}	g·cm^{-3}	g·cm^{-3}	g·cm^{-3}	g·cm^{-3}
288	1.29 ± 0.06	1.3146	0.0592	0.0655		
298	1.27 ± 0.03	1.2879	0.0306	0.0388		
308	1.24 ± 0.002	1.2600	0.0018	0.0109	0.0474	0.0564
318	1.21 ± 0.03	1.2309	−0.0323	−0.0667		
328	1.18 ± 0.06	1.2004	−0.0592	−0.0487		

[a] ρ_1, experimentally determined density; ρ_2, density from P-R equation; d_1, absolute error of experimental density; d_2, absolute error of density from P-R equation; s_1, standard deviation of experimental density; s_2, standard deviation of P-R equation density.

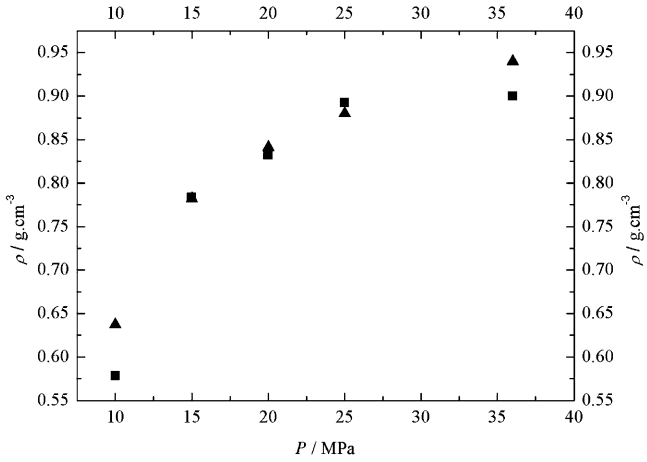

Figure 4. Density of $scCO_2$ calculated using the P-R equation and determined experimentally at 313 K and a range of pressures. ■, experimental data (density of our work); ▲, P-R equation data (density of P-R equation).

of the measured density was 0.1313 g·cm^{-1}, and the standard deviation of density calculated by P-R equation was 0.1153 g·cm^{-1}. The density from the P-R equation and the measured density for HFC-134a at 308 K at varying pressures are shown in Figure 5. The analysis of the density data is shown in Table 4. The standard deviations of the measured density and the density calculated from the P-R equation were 0.0429 and 0.0424 g·cm^{-1}, respectively. At the same temperature, the density curve from the P-R equation for HFC-134a is nearly parallel to the measured density curve. The two standard

Table 3. Standard Deviation and Absolute Error of $scCO_2$ Density Calculated Using the P-R Equation and Experimentally Determined at 313 K and a Range of Pressures[a]

P	ρ_1	ρ_2	d_1	d_2	s_1	s_2
MPa	g·cm^{-3}	g·cm^{-3}	g·cm^{-3}	g·cm^{-3}	g·cm^{-3}	g·cm^{-3}
10	0.57 ± 0.22	0.6373	−0.2189	−0.1789		
15	0.78 ± 0.01	0.7824	−0.0137	−0.0338		
20	0.83 ± 0.03	0.8412	0.0349	0.0250	0.1313	0.1153
25	0.89 ± 0.09	0.8802	0.0949	0.0640		
36	0.90 ± 0.10	0.9400	0.1029	0.1238		

[a] ρ_1, experimentally determined density; ρ_2, density from P-R equation; d_1, absolute error of experimental density; d_2, absolute error of density from P-R equation; s_1, standard deviation of experimental density; s_2, standard deviation of P-R equation density.

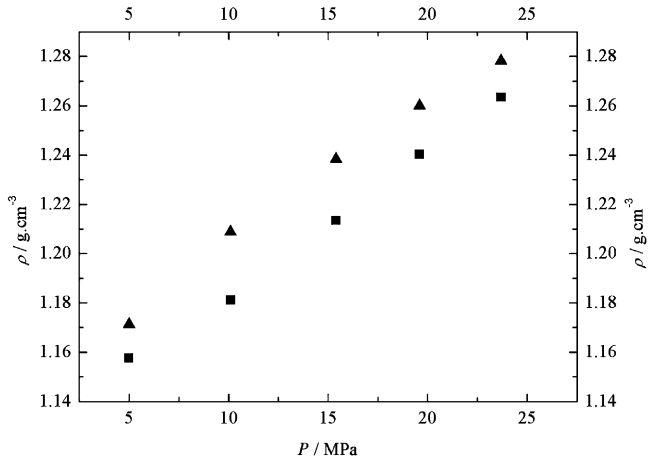

Figure 5. Density of HFC-134a calculated using the P-R equation and determined experimentally at 308 K and a range of pressures. ■, experimental data; ▲, P-R equation data.

Table 4. Standard Deviation and Absolute Error of HFC-134a Density Calculated Using the P-R Equation and Experimentally Determined at 308 K and a Range of Pressures[a]

P	ρ_1	ρ_2	d_1	d_2	s_1	s_2
MPa	g·cm^{-3}	g·cm^{-3}	g·cm^{-3}	g·cm^{-3}	g·cm^{-3}	g·cm^{-3}
5.0	1.15 ± 0.05	1.1712	−0.0536	−0.0601	0.0429	0.0424
10.1	1.18 ± 0.03	1.2088	−0.0299	−0.0225		
15.4	1.21 ± 0.002	1.2383	0.0023	0.0070		
19.6	1.24 ± 0.03	1.2600	0.0291	0.0287		
23.7	1.26 ± 0.05	1.2782	0.0523	0.0469		

[a] ρ_1, experimentally determined density; ρ_2, density from P-R equation; d_1, absolute error of experimental density; d_2, absolute error of density from P-R equation; s_1, standard deviation of experimental density; s_2, standard deviation of P-R equation density.

deviations are very similar, which indicates that the P-R equation is sufficiently accurate for our experimental calculation.

There are systematic errors between data calculated by the P-R equation and data obtained in our experimental calculation. We hypothesize that the systematic errors are from estimated errors on the pressure and temperature settings. The temperature was controlled during each experiment with a variation of (0.5 K). The pressure was measured using a pressure transducer (Beijing, Zhengkai, MCYB) and controlled during each experiment with a variation of (0.01 MPa). The other errors are from the experimentally determined weights.

Solubility Measurement. A static method coupled with gravimetric analysis was developed for measuring the solubility of L-proline in $scCO_2$ and HFC-134a.

Figure 6 reveals that the solubility of L-proline in HFC-134a increases with increase in temperature at constant pressure (19.6 MPa). The solubility of L-proline in $scCO_2$ at 20 MPa and

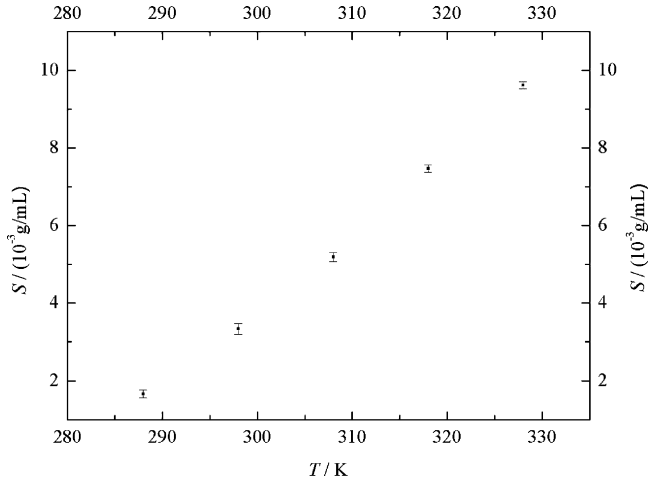

Figure 6. Solubility of L-proline in HFC-134a at 19.6 MPa and a range of temperatures. Error bars use the 95 % confidence interval, which corresponds to approximately 3 standard deviations taken from triplicate runs. ■, solubility data.

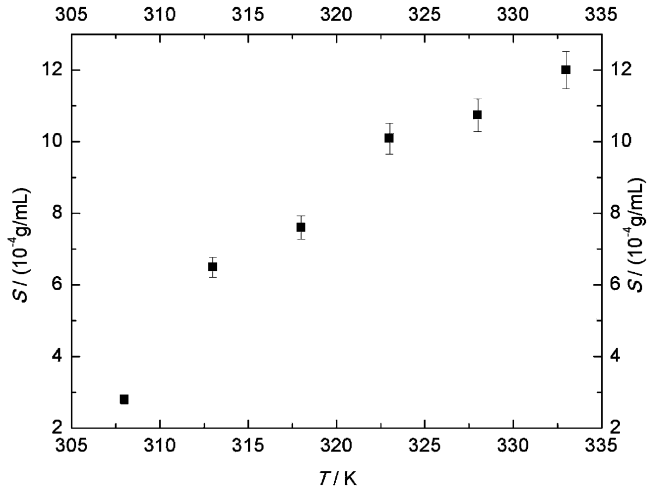

Figure 7. Solubility of L-proline in $scCO_2$ at 20 MPa and a range of temperatures. Error bars use the 95 % confidence interval, which corresponds to approximately 3 standard deviations taken from triplicate runs. ■, solubility data.

varying temperature is shown in Figure 7. The error bars correspond to one standard deviation calculated from three replicate measurements done at each temperature and pressure. The solubility increased with increasing temperature at constant pressure for L-proline in HFC-134a and $scCO_2$, because when the temperature increases, compared with the decrease of density, the increase of vapor pressure is the most important factor. This explanation applies to both CO_2 and HFC-134a solvents.

The solubility of L-proline in HFC-134a at a fixed temperature (308 K) and varying pressure (5 MPa to 25 MPa) is given in Figure 8. The solubility of L-proline in $scCO_2$ at a fixed temperature (313 K) and varying pressure (10 MPa to 36 MPa) is given in Figure 9. The error bars correspond to one standard deviation calculated from triplicate measurements at each temperature and pressure. The solubility of a solute in a fluid depends strongly on the density and increases with increase in density hence with increase in pressure. This is in accord with conventional wisdom that the density of a supercritical fluid must increase in order to increase the solubility and extraction efficiency.[34] Considering the thermodynamic view, at a given temperature the Hildebrand formula $\Delta H_M = V(\delta_1\text{-}\delta_2)$ predicts

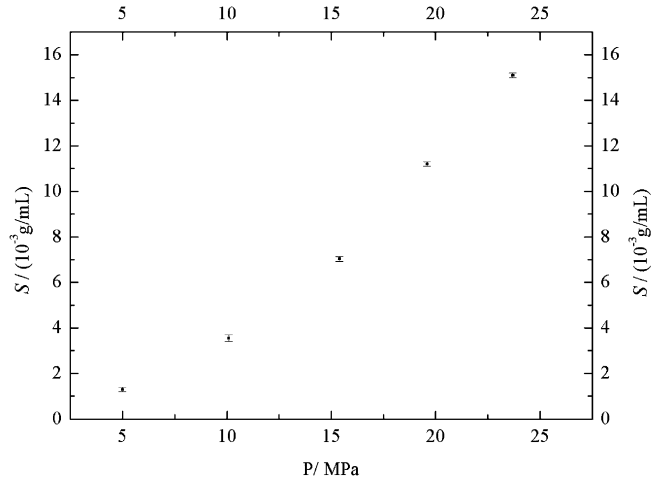

Figure 8. Solubility of L-proline in HFC-134a at 308 K and a range of pressures. Error bars use the 95 % confidence interval, which corresponds to approximately 3 standard deviations taken from triplicate runs. ■, solubility data.

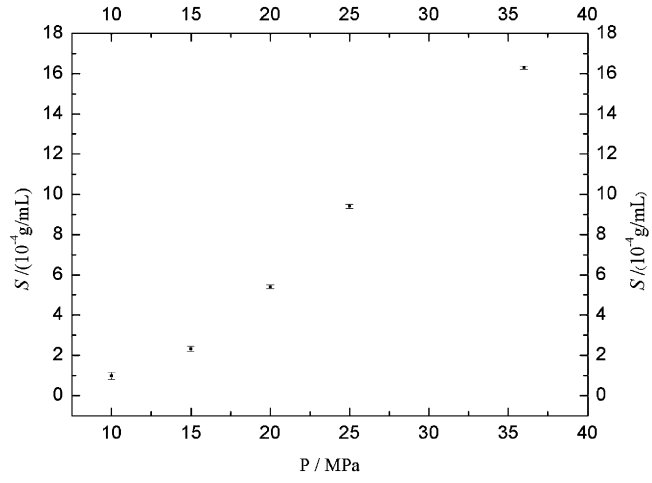

Figure 9. Solubility of L-proline in $scCO_2$ at 313 K and a range of pressures. Error bars use the 95 % confidence interval, which corresponds to approximately 3 standard deviations taken from triplicate runs. ■, solubility data.

Table 5. Experimental Solubility Data for L-Proline in $scCO_2$ and HFC-134a at 20 MPa and 308 K, 318 K, and 328 K[a]

		CO_2	HFC-134a	CO_2	HFC-134a
P/MPa	*T*/K	*m*/g	*m*/g	$S \times 10^4$ /g·mL^{-1}	$S \times 10^4$ /g·mL^{-1}
20	308	0.0120	0.2232	2.79	51.90
	318	0.0327	0.3211	7.60	74.70
	328	0.0462	0.4134	10.74	96.20

[a] *m*, amount dissolved; *S*, solubility

that if the solubility parameters of a fluid solvent δ_1 and a solute δ_2 are almost equal in magnitude, the enthalpy of mixing, ΔH_M, is small and the solute should dissolve in the solvent. The results indicate that at low pressure (10 MPa to 15 MPa) the increasing trend of solubility with increase in pressure is slow, while at higher pressure (15 MPa to 20 MPa) the increasing trend is fast. Pressure has the predominant influence on the density of a supercritical fluid; the density increases with increasing pressure at constant temperature.

The solubilities of L-proline in $scCO_2$ and HFC-134a at the same pressure are listed in Table 5. Under the same conditions, the solubility of L-proline in HFC-134a is much higher than in $scCO_2$. The results indicate that HFC-134a is a more polar

solvent than $scCO_2$ for dissolving the polar compound. Because $scCO_2$ is a nonpolar solvent with weak van der Waals forces, between solute and $scCO_2$ there are dipole−quadrupole forces that inhibit dissolution of the solute.[35] Consequently, polar solutes cannot easily dissolve in $scCO_2$. However, HFC-134a is a polar solvent that has a strong solvent power for polar solutes. Since the dipole−dipole force between polar solute and HFC-134a promotes dissolution, the solubility of L-proline in HFC-134a is higher than in $scCO_2$.[32]

Conclusion

A static method coupled with gravimetric analysis was developed for measuring the solubility of L-proline in $scCO_2$ and HFC-134a fluids. The solubility increases with increasing temperature and pressure for $scCO_2$ and HFC-134a. The solubility of the polar solute in HFC-134a was found to be much higher than in the most commonly used supercritical solvent, that is, CO_2. The densities of CO_2 and HFC-134a calculated using the P-R equation are close to the experimental values in a wide range of temperatures and pressures.

Literature Cited

(1) List, B. The ying and yang of asymmetric aminocatalysis. *Chem. Commun.* **2006**, 819–824.

(2) (a) Kočovský, P.; Malkov, A. V. Organocatalysis in organic synthesis. *Tetrahedron* **2006**, *62*, 255–255. (b) Marigo, M.; Jørgensen, K. A. Organocatalytic direct asymmetric a-heteroatom functionalization of aldehydes and ketones. *Chem.Commun.* **2006**, 2001–2011.

(3) (a) Sabitha, G.; Fatima, N.; Reddy, E. V.; Yadav, J. S. First examples of proline-catalyzed domino Knoevenagel/Hetero-Diels-Alder/Elimination reactions advanced synthesis & catalysis. *Adv. Synth. Catal.* **2005**, *347*, 1353–1355. (b) Chen, S. H.; Hong, B. C.; Su, C. F.; Sarshar, S. An unexpected inversion of enantioselectivity in the proline catalyzed intramolecular Baylis-Hillman reaction. *Tetrahedron Lett.* **2005**, *46* (51), 8899–8903. (c) Chowdari, N. S.; Ramachary, D. B.; Barbas, C. F. III. Organocatalysis in ionic liquids: highly efficient L-proline-catalyzed direct asymmetric mannich reactions involving ketone and aldehyde nucleophiles. *Synlett.* **2003**, 1906–1909. (d) Notz, W.; Tanaka, F.; Watanabe, S.; Chowdari, N. S.; Turner, J. M.; Thayumanavan, R.; Barbas, C. F., III. The direct organocatalytic asymmetric mannich reaction: unmodified aldehydes as nucleophiles. *J. Org. Chem.* **2003**, *68*, 9624–9634.

(4) (a) Chandrasekhar, S.; Reddy, N. R.; Sultana, S. S.; Narsihmulu, Ch.; Reddy, K. V. L-Proline catalysed asymmetric aldol reactions in PEG-400 as recyclable medium and transfer aldol reactions. *Tetrahedron* **2006**, *62*, 338–345. (b) Bernard, A. M.; Frongia, A.; Guillot, R.; Piras, P. P.; Secci, F.; Spiga, M. L-Proline-catalyzed direct intermolecular asymmetric aldol reactions of 1-phenylthiocycloalkyl carboxaldehydes with ketones. Easy access to spiro- and fused-cyclobutyl tetrahydrofurans and cyclopentanones. *Org. Lett.* **2007**, *9* (3), 541–544.

(5) Pihko, P. M.; Laurikainen, K. M.; Usano, A.; Nyberg, A. I.; Kaavi, J. A. Effect of additives on the proline-catalyzed ketone-aldehyde aldol reactions. *Tetrahedron* **2006**, *62*, 317–328.

(6) Bellis, E.; Kokotos, G. Proline-modified poly(propyleneimine) dendrimers as catalysts for asymmetric aldol reactions. *J. Mol. Catal. A: Chem.* **2005**, *241*, 166–174.

(7) Eckert, C. A.; Knutson, B. L.; Debenedetti, P. G. Supercritical fluids as solvents for chemical and materials processing. *Nature* **1996**, *383*, 313–318.

(8) Cooper, A. I. Polymer synthesis and processing using supercritical carbon dioxide. *J. Mater. Chem.* **2000**, *10*, 207–234.

(9) Dillow, A. K.; Yun, S. L.; Suleiman, D. S.; Boatright, D. L.; Liotta, C. L.; Eckert, C. A. Kinetics of a phase-transfer catalysis reaction in supercritical fluid carbon dioxide. *Ind. Eng. Chem. Res.* **1996**, *35*, 1801–1806.

(10) Holmes, J. D.; Steytler, D. C.; Rees, G. D.; Robinson, B. H. Bioconversions in a water-in-CO_2 microemulsion. *Langmuir* **1998**, *14*, 6371–6376.

(11) Sundararajan, N.; Yang, S.; Ogino, K.; Valiyaveettil, S.; Wang, J.; Zhou, X.; Ober, C. K.; Obendorf, S. K.; Allen, R. D. Supercritical CO_2 processing for submicron imaging of fluoropolymers. *Chem. Mater.* **2000**, *12*, 41–48.

(12) Ji, M.; Chen, X.; Wai, C. M.; Fulton, J. L. Synthesizing and dispersing silver nanoparticles in a water-in-supercritical carbon dioxide microemulsion. *J. Am. Chem. Soc.* **1999**, *121*, 2631–2632.

(13) Ohde, H.; Ohde, M.; Bailey, F.; Kim, H.; Wai, C. M. Water-in-CO_2 microemulsions as nanoreactors for synthesizing CdS and ZnS nanoparticles in supercritical CO_2. *Nano Lett.* **2002**, *2*, 721–724.

(14) Ohde, H.; Rodriguez, J. M.; Ye, X. R.; Wai, C. M. Synthesizing silver halide nanoparticles in supercritical carbon dioxide utilizing a water in-CO_2 microemulsion. *Chem. Commun.* **2000**, *23*, 2353–2354.

(15) Dong, X.; Potter, D.; Erkey, C. Synthesis of CuS nanoparticles in water-in-carbon dioxide microemulsions. *Ind. Eng. Chem. Res.* **2002**, *41*, 4489–4493.

(16) Lim, J. S.; Park, J. Y.; Yoon, C. H.; Lee, Y. W.; Yoo, K. P. Cloud points of poly(L-lactide) in HCFC-22, HFC-23, HFC-32, HFC-125, HFC-143a, HFC-152a, HFC-227ea, dimethyl ether (DME), and HCFC-22 + CO_2 in the supercritical state. *J. Chem. Eng. Data* **2004**, *49*, 1622–1627.

(17) Eastoe, J.; Gold, S. Self-assembly in green solvents. *Phys. Chem. Chem. Phys.* **2005**, *7*, 1352–1362.

(18) Olsen, S. A.; Tallman, D. E. Conductivity and voltammetry in liquid and supercritical halogenated solvents. *Anal. Chem.* **1996**, *68*, 2054–2061.

(19) Abbott, A. P.; Eardley, C. A.; Harper, J. C.; Hop, E. G. Electrochemical investigations in liquid and supercritical 1,1,1,2-tetrafluoroethane (HFC-134a) and difluoromethane (HFC-32). *J. Electroanal. Chem.* **1998**, *457*, 1–4.

(20) Tackson, K.; Fulton, J. L. Microemulsions in supercritical hydrochlorofluorocarbons. *Langmuir* **1996**, *12*, 5289–5295.

(21) Butz, N.; Porte, C.; Courrier, H.; Krafft, M. P.; Vandamme, Th. F. Reverse water-in-fluorocarbon emulsions for use in pressurized metered-dose inhalers containing hydrofluoroalkane propellants. *Int. J. Pharm.* **2002**, *238*, 257–269.

(22) Eastoe, J.; Thorpe, A. M.; Eastone, J.; Dupont, A.; Heenan, R. K. Microemulsion formation in 1,1,1,2-tetrafluoroethane (134a). *Langmuir* **2003**, *19*, 8715–8720.

(23) Bush, D.; Echert, C. A. Prediction of solid-fluid equilibria in supercritical carbon dioxide using linear solvation energy relationships. *Fluid Phase Equilib.* **1998**, *150−151*, 479–492.

(24) Ozcan, A. S.; Clifford, A. A.; Bartle, K. D. Solubility of disperse dyes in supercritical carbon dioxide. *J. Chem. Eng. Data* **1997**, *42*, 590–592.

(25) Joung, S. N.; Yoo, K. Solubility of disperse anthraquinone and azodyes in supercritical carbon dioxide at 313.15 to 393.15 K and from 10 to 25 MPa. *J. Chem. Eng. Data* **1998**, *43*, 9–12.

(26) Lee, J. W.; Min, J. M.; Bae, H. K. Solubility measurement of disperse dyes in supercritical carbon dioxide. *J. Chem. Eng. Data* **1999**, *44*, 684–687.

(27) Yamini, Y.; Bahramifar, N. Solubility of polycyclic aromatic hydrocarbons in supercritical carbon dioxide. *J. Chem. Eng. Data* **2000**, *45*, 53–56.

(28) Chrastil, J. Solubility of solids and liquids in supercritical gases. *J. Phys. Chem.* **1982**, *86*, 3016–3021.

(29) Peng, D.; Robinson, D. B. A new two-constant equation of state. *Ind. Eng. Chem. Fundam.* **1976**, *15*, 59–64.

(30) Sherman, G.; Shenoy, S.; Weiss, R. A.; Erkey, C. A Static Method Coupled with Gravimetric Analysis for the Determination of Solubilities of Solids in Supercritical Carbon Dioxide. *Ind. Eng. Chem. Res.* **2000**, *39*, 846–848.

(31) Liu, Z. T.; Liu, L.; Wu, J.; Song, L. P.; Gao, Z.; Dong, W.; Lu, J. Solubility and phase behaviors of AOT analogue surfactants in 1,1,1,2-tetrafluoroethane and supercritical carbon dioxide. *J. Chem. Eng. Data* **2006**, *51*, 2045–2050.

(32) Liu, Z. T.; Wu, J.; Liu, L.; Sun, C.; Song, L. P.; Gao, Z.; Dong, W.; Lu, J. Solubilities of AOT analogues surfactants in supercritical CO_2 and HFC-134a fluids. *J. Chem. Eng. Data* **2006**, *51*, 1761–1768.

(33) Valderrama, J. O.; Alvarez, V. H. Phase equilibrium in supercritical CO_2 mixtures using a modified Kwak-Mansoori mixing rule. *AIChE J.* **2004**, *50*, 480–488.

(34) Miller, D. J.; Hawthorne, S. B. Determination of solubilities of organic solutes in supercritical CO_2 by on-Line flame ionization detection. *Anal. Chem.* **1995**, *67*, 273–279.

(35) Abbott, A. P.; Corr, S.; Durling, N. E.; Hope, E. G. Solubility of substituted aromatic hydrocarbons in supercritical difluoromethane. *J. Chem. Eng. Data* **2002**, *47*, 900–905.

Received for review December 31, 2008. Accepted March 30, 2009. The authors gratefully acknowledge the financial support of the Specialized Research Fund for the Doctoral Program of Higher Education (20070718003) and the Natural Science Foundation of Shaanxi Province (2007B07).

JE801009Z